Round and Extracted Nb_3Sn Strand Tests for LARP Magnet R&D*

Emanuela Barzi, Rodger Bossert, Shlomo Caspi, Dan Dietderich, Paolo Ferracin, Arup Ghosh, Daniele Turrioni, Ryuji Yamada, and Alexander V. Zlobin

Abstract—**The first step in the magnet R&D of the U.S. LHC Accelerator Research Program (LARP) is fabrication of technology quadrupoles TQS01 and TQC01. These are two-layer magnets which use cables of same geometry made of 0.7 mm MJR Nb_3Sn. Through strand billet qualification and tests of strands extracted from the cables, predictions of magnet performance are made. Measurements included the critical current, I_c, using the voltage-current (VI) method at constant field, the stability current, I_S, as the minimal quench current obtained with the voltage-field (VH) method at constant current in the sample, and RRR. Magnetization was measured at low and high fields to determine the effective filament size and to detect flux jumps. Effects of heat treatment duration and temperature on I_c and I_S were also studied. The Nb_3Sn strand and cable samples, the equipment, measurement procedures, and results are described. Based on these results, strand specifications were formulated for next LARP quadrupole models.**

Index Terms—**Critical current density, magnetic instability, Nb_3Sn, Rutherford cable.**

I. Introduction

LARP Technology Quadrupole (TQ) and Subscale Quadrupole (SQ) magnet design is presently based on 0.7 mm Nb_3Sn strands. On account of the strands that were available to BNL, FNAL and LBNL, in the original plan TQC01 [1] had to be made of Modified Jelly Roll (MJR) and TQS01 [2] of Restack Rod Process (RRP), both with a 54/61 subelement design, *i.e.* 54 subelements in a 61-stack billet. However, due to the larger critical current density, J_c, of the RRP strand, which makes it proportionally more unstable [3], [4], eventually the decision was made to use MJR for both TQ's and also for SQ02. In the meantime, the LARP Materials Group focuses on improving magnetic stability of state-of-the-art Nb_3Sn strands. Several groups worked on this topic [5]–[8], and it was experimentally shown that an effective filament diameter, d_{eff}, of excessive size reduces the critical current, I_c, at low field to $\leq$20% of its expected value. Collaborating with strand manufacturers to reduce d_{eff} is therefore important.

Manuscript received September 20, 2005. This work was supported by the U.S. Department of Energy.

E. Barzi, R. Bossert, D. Turrioni, R. Yamada, and A. V. Zlobin are with Fermi National Accelerator Laboratory, Batavia, IL 60510 USA (e-mail: barzi@fnal.gov).

S. Caspi and D. Dietderich are with Lawrence Berkeley National Laboratory, Berkeley, CA 94720 USA (e-mail: drdietderich@lbl.gov; s_caspi@lbl.gov).

A. Ghosh is with Brookhaven National Laboratory, Upton, NY 11973 USA (e-mail: aghosh@bnl.gov).

Digital Object Identifier 10.1109/TASC.2006.870785

*This work was supported by the U.S. Department of Energy under Contract No. DE-AC02-05CH11231.

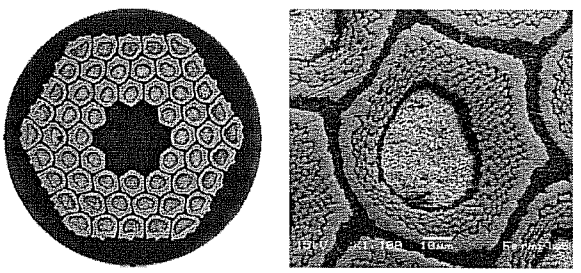

Fig. 1. Left: optical microscopy of an unreacted 0.7 mm MJR strand. Right: SEM zoom in a subelement.

The Conductor Development Program (CDP) is contributing in this endeavor. The most promising strand design is presently the RRP with larger number of restacks. The RRP, contrary to MJR, has scale-up potential albeit approximately same cost.

In order to select a cable design, extensive R&D was performed by fabricating cables at LBNL with various numbers of strands and keystone angles. Both high field I_c degradation and low field stability were studied and measured. Eventually a 27-strand cable with a 1 degree keystone angle was chosen as a conservative approach. Heat treatment (HT) optimization was done to meet the two conflicting requests of high I_c at high field, and good stability (high I_s) at low fields. Optimization was carried out on both round strands and strands extracted from cables, as the latter typically behave quite differently. Short sample limit predictions were measured and calculated for the newly fabricated and heat treated SQ02 using witness strand and cable samples. Finally, the work done so far allowed to formulate specifications for the next LARP coils.

II. Strand and Cable Description

Three billets of 0.7 mm multifilamentary MJR strands by Oxford Superconducting Technology (OST) were used for this work. Fig. 1 shows a strand cross section. The strand properties as measured by OST after applying two different heat treatments are summarized in Table I.

Short samples of 26, 27 and 28 strand cables with two different keystone angles were made at LBNL (Table II). Cables 910 were made out of billet 205 (length A), and cables 913 out of billet 206 (length C). The cross section of a TQ cable with 27 strands and 1 degree keystone angle is shown in Fig. 2. Table II also includes a 20-strand cable, ID 926, which was used to wind SQ02. Cable 926 was a blend of all three billets 205, 206 and 208. The packing factor, PF, in Table II was calculated as the

TABLE I
MJR STRAND PROPERTIES AS MEASURED BY OST

Billet ID	Ore 205	Ore 206	Ore 208
Diameter, mm	0.703 ± 0.002	0.703 ± 0.002	0.703 ± 0.002
No. subelements	54 in 61-stack	54 in 61-stack	54 in 61-stack
Cu, %	46.7 ± 0.2	47.3 ± 0.3	47.4 ± 0.2
Right-handed twist, mm	12	12	13
No. lengths	10	17	13
Total length, m	8517	8887	7514
I_c(12 T) w/HT-1[a], A	423 ± 11	415 ± 1	439 ± 5
RRR w/HT-1[a]	5	5	5
I_c(12 T) w/HT-2[b], A	405 ± 10	384 ± 2	424 ± 4
RRR w/HT-2[b]	21 ± 11	42 ± 6	42 ± 7

[a] HT-1 was 100 h at 210°C, 48 h at 340°C, 180 h at 650°C.
[b] HT-2 was 100 h at 210°C, 48 h at 340°C, 90 h at 650°C.

TABLE II
MJR CABLE DESCRIPTION

Cable ID	Strand No.	Pre-anneal dimensions, mm x mm	Pre-anneal angle, degree	Re-roll dimensions, mm x mm	Re-roll Angle, degree	PF, %
910-A	28	10.088 x 1.323	0.996	10.039 x 1.269	1.297	88
910-B	27	10.043 x 1.313	0.964	10.024 x 1.257	1.312	85.8
910-E	26	10.02 x 1.308	1.377	10.011 x 1.255	1.357	84.1
913-A	28	10.071 x 1.281	0.996	10.033 x 1.274	1.019	87.7
913-B	27	10.039 x 1.272	1.05	10.012 x 1.267	1.047	85.2
913-C	26	10.00 x 1.271	1.139	10.008 x 1.262	0.839	83.8
926	20	7.837 x 1.29	0	7.793 x 1.276	0	80.8

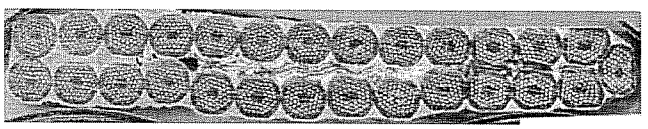

Fig. 2. Cross section of a TQ production cable.

ratio of the cross section occupied by the strands to the overall cross section of the cable after re-rolling.

III. REACTION AND TEST PROCEDURES

A. Comparison of Reaction and Test Procedures

The reaction and test procedures presently followed by the three Labs are summarized in Table III. The I_c was determined from the VI curve using the $10^{-14}\Omega\cdot$m resistivity criterion. The I_c measurement uncertainty is typically within ±1% at 4.2 K and 12 T. VH tests involved ramping to a fixed transport current, and sweeping the field up and down with ramp rates of 5 to 17 mT/s in the field range 0-4-0 T. If no quench was observed the current was increased and the test repeated. This test was done to determine the minimum quench current, or stability current, I_S, in the presence of a magnetic field variation.

B. Comparison of Test Results (Round Robin)

For an accurate representation of the data obtained at BNL, FNAL and LBNL, a round robin test run was performed. To distinguish the effects of reaction from those due to testing, six samples of 205 strand (length H) were heat treated together at BNL using HT-4 in Table IV, and distributed among the three Labs for testing. To measure the effect of a bonding agent like STYCAST, each Lab tested the samples with and without STYCAST. Test results at 4.2 K averaged over two samples (when data were available) are shown in Table V.

The I_c reproducibility obtained at 12 T when testing similar samples was better than 2.5% at the three Labs. This is consistent with I_c uniformity in previously measured MJR strands [10]. The I_S reproducibility was within 20%. In FNAL and BNL tests, STYCAST did not appear to produce a systematic effect

TABLE III
REACTION AND TEST PROCEDURES

Reaction	LBNL	FNAL*	BNL
Reaction barrel/ rings	Ti-6Al-4V/ Ti-6Al-4V	Ti-6Al-4V/ Ti-6Al-4V	304 SS/ No rings
Sn leaks prevention	Seal ends with acetylene-oxygen torch	Strands have 12" tails, ends peened	Strands have 12" tails, ends peened
Heat treatment atmosphere	Argon	Argon	Vacuum
Test	**LBNL**	**FNAL**	**BNL**
Max. field, T	14	15	11.5
Max sample current, A	2000	1800	1500 for VI 1200 for VH
Test barrel	Same reaction barrel/ Remove Ti rings	Same reaction barrel/ Remove Ti rings	Transfer to Ti-6Al-4V barrel, Cu is grooved
Wire to barrel bonding	Blue STYCAST	None	None
Barrel to probe mounting	Solder contact	Pressure contact for P1 Solder contact for P2	One-piece Cu-Ti-Cu unit
Voltage taps	2 pairs on sample at 5 and 7 turns	2 pairs on sample at 5 and 7 turns	2 pairs on sample at 5 and 7 turns
Thermometry in bath	Carbon glass	Cernox	Carbon glass
Thermometry on sample	None	None for P1 Cernox for P2	None
Wire to Cu	Pb-Sn solder	Pb-Sn solder	Pb-Sn solder

*Under the FNAL column, ì P1î stands for Probe 1, and ì P2î for Probe 2.

TABLE IV
LAST[a] STEP OF HEAT TREATMENT CYCLES

HT	Ramp rate, °C/h	Temperature, °C	Duration, h
1[a]	50	665	72
2[a]	50	650	72
3[b]	75	640	60
4[a]	50	650	48
5[a]	50	635	72
6[a]	50	635	48
7[a]	50	680	72

[a] First steps were 48 h at 210°C, and 48 h at 400°C.
[b] First steps were 48 h at 210°C, and 48 h at 340°C.

TABLE V
ROUND ROBIN TEST RESULTS

Strand ID I_c, A at	14 T	13 T	12 T[a]	10 T	8 T	Is, A	RRR
FNAL	245±2	317±2	402±1	612±2		980±170	211±11
FNAL w/STY	252±3	320±2	406	616	911	975±110	
BNL			[415]±7	621±8	905±9	1100±140	189±66
BNL w/STY			[421]±1	629±3	909	1100	
LBNL	220	288	366			>1210	
LBNL w/STY	243	316±10	401±6	608±10			272±7

[a] Values in square parentheses were parameterized using [9] with $T_{c0}(\varepsilon)$=18 K and $B_{c20}(\varepsilon)$=25 T.

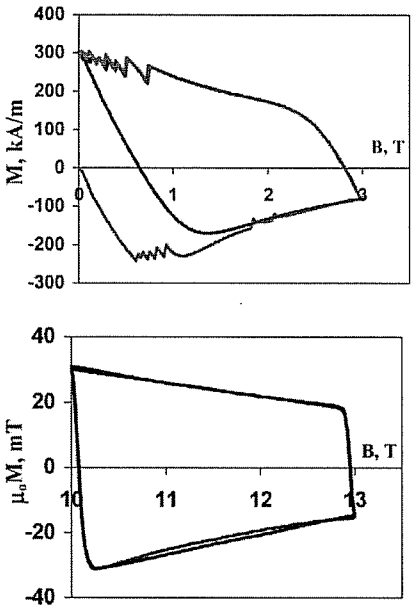

Fig. 3. Magnetization curves per total volume of a 208-A strand at low (top) and high field (bottom).

on I_S. In the LBNL tests, the I_c at 12 T of the sample tested after applying STYCAST increased by $\sim$ 10%. The difference in I_c test results between BNL and FNAL was $\sim$3% at 12 T down to zero at 8 T. The difference in I_c results of the samples tested at 12 T with STYCAST was less than 5% among the three Labs. The difference in the average I_S results was $\sim$20–25% among the three Labs.

IV. Billets Characterization

Samples out of billets 205 and 206 were characterized for transport properties. Both magnetization (see Fig. 3) and critical current were tested at FNAL for a sample out of billet 208-A, heat treated using HT-3 in Table IV. Magnetization at 12 T per total strand volume was (41.8 $\pm$ 1) mT. The I_c at 12 T was 395 A. The resulting d_{eff} was (79.9 $\pm$ 1.8) μm. One can see flux jumps in the magnetization curves at low fields.

V. Cables Qualification

A. *High Field* I_c *Degradation*

The results of cabling degradation as the critical current of the extracted strand normalized to that of the virgin strand at 4.2 K are shown in Figs. 4 and 5 for cable series 910 and 913 as a function of magnetic field and for a number of different heat treatments (see also Table IV). The cabling degradation was less than 6% when measured at BNL and LBNL, and up to 14% as measured at FNAL. This might be due to a different method of preparing and/or testing extracted samples, and is not understood sufficiently. Fig. 6 shows I_c degradation at 12 T for both cable series as a function of the number of strands. These I_c measurements indicate no systematic variation with the number of strands used to make the cable or with the cable keystone angle.

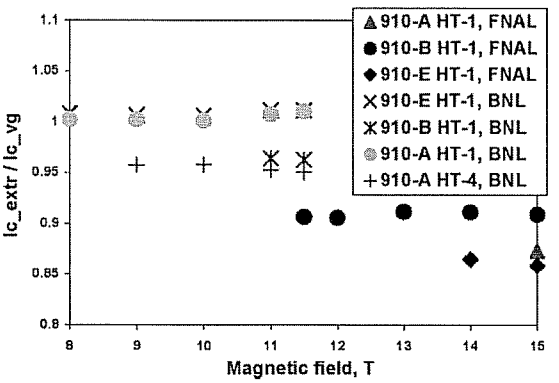

Fig. 4. Cabling degradation at 4.2 K for cable series 910 (1.3 degree) as a function of magnetic field as measured by BNL and FNAL.

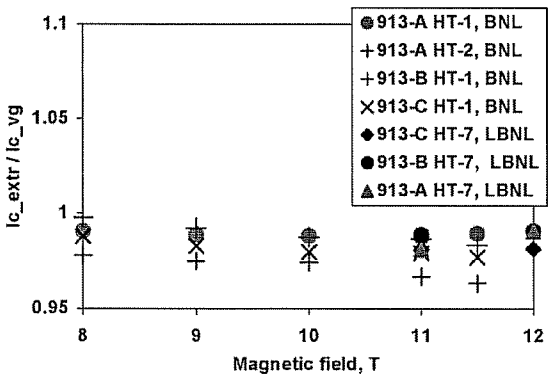

Fig. 5. Cabling degradation at 4.2 K for cable series 913 (1 degree) as a function of magnetic field as measured by BNL and LBNL.

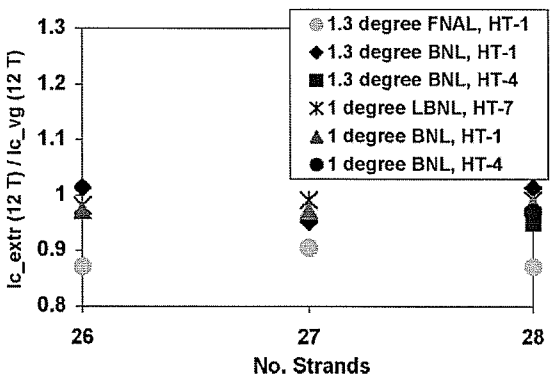

Fig. 6. Cabling degradation at 4.2 K for both cable series 910 and 913 at 12 T as measured, or parameterized using [10], at the three Labs.

B. *Low Field Stability*

The stability current, I_S, is shown for round samples and for strands extracted from cable series 910 and 913 as measured at 4.2 K at the three Labs in Fig. 7. In about 60% of the cases, these currents are of the same order as the critical currents at 12 T, and are likely due to the low RRR (between 10–15 at BNL, and between 6–13 at LBNL) produced by HT-1 and 7. The largest difference in the average I_S results was $\sim$ 30% among the three

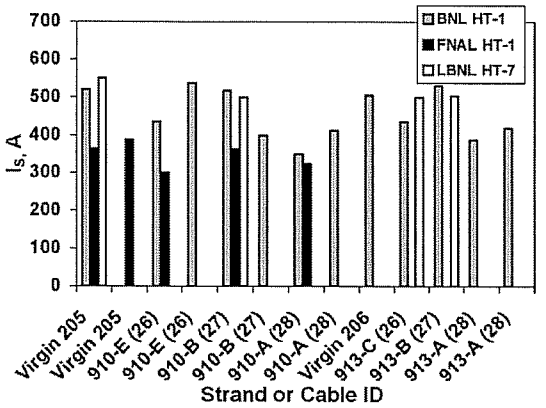

Fig. 7. I_S for round samples and for strands extracted from cable series 910 and 913 as measured at 4.2 K at the three Labs.

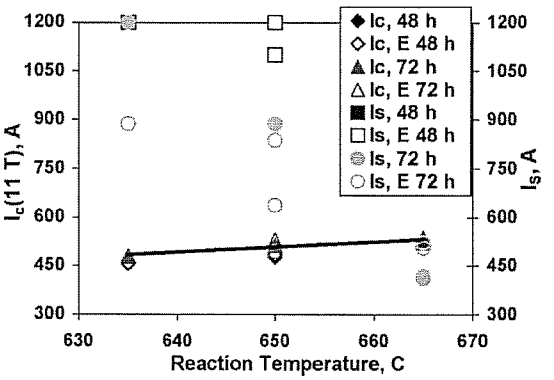

Fig. 8. I_c (11 T) (shown with line) and I_S as measured at 4.2 K at BNL for round and extracted ("E" in legend) strands as a function of time and reaction temperature.

TABLE VI
CABLE TEST RESULTS AT SELF-FIELD

HT	Cable ID	Impregnation	Splice R, nΩ	Cable Ave. I_q, A	Cable Min. I_q, A	Ave. I_q/ strand, A	Min. I_q/ strand, A
SQ02	926	Y	2.9	18362	17965	918	898
"	"	N	4.8	18874	17846	943	892

TABLE VII
SQ02 WITNESS SAMPLE TEST RESULTS

Strand ID	I_c, A at	13 T	12 T	11 T	10 T	8 T	I_S, A	RRR
205-J, FNAL		292	371				1100	135
206-N, FNAL		300	390		594	860	1200	
206-N, BNL			[391]	481	590	872	1100	203
208-F1, BNL			[413]	511	626	914	>1200	
Extr. 208-J, LBNL		298	380	474	584		1300	158

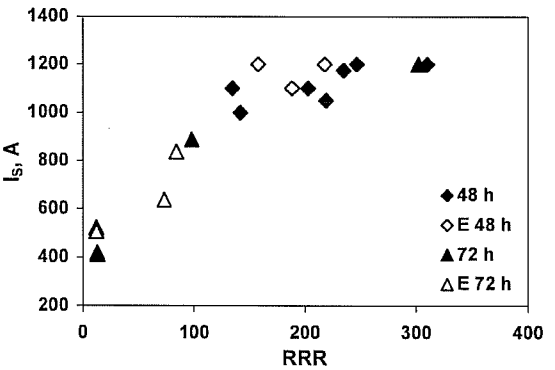

Fig. 9. I_S as measured at 4.2 K at the three Labs for round and extracted ("E" in legend) strands as a function of RRR. Black data points represent samples tested at BNL that did not quench up to BNL 1200 A power supply limit.

Labs. As can be seen from Fig. 7, no systematic variation with the number of strands in the cable or with the keystone angle was observed for I_S. This was true also for the RRR.

C. *Cable Tests*

Cables quench currents were measured at self-field with a SC transformer [11]. An example of the results obtained for the 926 cable witnesses used in the SQ02 reaction is given in Table VI. A cable sample was tested bare, and one was tested impregnated. All samples showed low I_q at self-field with respect to their expected I_c. Cables at self-field quench at currents that are systematically lower than in strands. This can be seen for instance in the homogeneous comparison of the cable test results in Table VI with the strand test results in Table VII, as both these strands and cables were used as witnesses in the same SQ02 reaction cycle.

VI. OPTIMIZATION OF REACTION CYCLE

To establish a suitable heat treatment schedule for the first TQ and SQ magnets, heat treatment optimization cycles that provide good I_c and I_S were searched. Table IV gives a list of cycles that were studied. The I_c(11 T) and the I_S as measured at 4.2 K for both round and extracted ("E" in legend) strands at BNL are plotted in Fig. 8 as a function of time and temperature of reaction. Strands were extracted from 28-strand cables 910-A and 913-A. I_S data points at 1200 A represent samples that did not quench up to power supply limit. The different I_S values at 650° C were obtained for the two different cables, with the largest value being associated to the 1.3 degree cable 910-A in both cases. One can see that whereas the I_c increases by only ~11 to 12% over a 15 to 30° C temperature increase, the I_S can decrease by a factor of three or larger over the same temperature range.

The I_S as measured at 4.2 K for both round and extracted ("E" in legend) strands at the three Labs is plotted in Fig. 9 as a function of RRR. The black data points represent samples reaching 1200 A (BNL power supply limit) without quenching. Nevertheless, one can see that around 200 in RRR, I_S flattens.

VII. PREDICTION OF SHORT SAMPLE LIMIT

Witness samples are used to predict short sample limits for coils. Ideally witnesses should be able to predict both high field and low field (i.e. stability) performance. In the case of SQ02, six round strands (two from each billet) and three extracted strands (one from each billet) were included in the oven during reaction of the coils. The actual reaction schedule was 47 h at 207° C, 46 h at 395° C, and 47.5 h at 638° C, with temperatures being measured with K-type thermocouples. This cycle was chosen to preserve as much as possible I_S (see Fig. 8). The samples were distributed among the three Labs for testing. Test

TABLE VIII
STRAND SPECIFICATIONS

Technology	Ternary RRP Nb_3Sn
Diameter, mm	0.7 – 1.0
J_c(12 T), A/mm^2	≥ 2400
d_{eff}, μm	< 60
I_S, A	> 1200 A
Cu, %	50 ± 2
RRR	≥ 100
RH twist, mm	15 ± 1
Piece length, m	≥ 350

results are shown in Table VII at magnetic fields where data exist for at least two Labs. Between square parentheses are values for I_c (12 T) that were parameterized using [9] when direct measurements were not available.

Based on the extracted strand results, SQ02 was expected to reach a maximum magnetic field of 10.9 T at a current of 9800 A, and a gradient of 82 T/m. When tested, SQ02 reached its maximum current of 9590 A in the second thermal cycle [12]. In the prediction three effects, which would all reduce the expected I_c, were not considered. A temperature effect due to the coil being tested at 4.3 K, a billet blend effect due to the short sample limit being calculated for the best performing billet (ID 208), and a strain effect due to the samples being tested on Ti-alloy barrels (the tensile strain can increase the inherent I_c). The I_c cabling degradation as measured at 12 T for the round and extracted strands from the same billet (ID 208) was 8%. The I_S was ≥1100 A for all strand witnesses, and >900 A when derived from cable tests (Table VI). The RRR of the virgin strands ranged from 135 to 206, and that of the extracted strands from 128 to 167.

VIII. STRAND SPECIFICATIONS FOR FUTURE MODELS

Specifications for the upcoming LARP magnets are shown in Table VIII. To avoid instabilities in magnet performance, a moderate strand J_c and high RRR were required. I_S was also included in the specs to control strand stability.

IX. SUMMARY

A MJR strand of 0.7 mm diameter is being used for the first model magnets in the LARP Magnet R&D program. This strand was extensively studied both at the round level, and after making several rectangular and keystoned cables. Round samples were tested at BNL, FNAL and LBNL to verify consistency, as each Lab has its own equipment and procedures when performing heat treatments and tests. A good consistency was found for I_c and I_S among the three Labs. This consistency will be periodically checked in the future.

Effects of cabling were measured using strands extracted from the prototype cables, which included cables made of 26, 27 and 28 strands, with a 1 degree and 1.3 degree keystone angles. Cabling produces filament deformation, which worsens magnetic instability, and sometimes barrier shearing, which causes Sn-leakages and worsens RRR. These effects do not always have substantial consequences on the I_c, but the I_S can be more heavily affected. No strong correlation was found in the I_c and I_S measurements with the number of strands used to make the cable or with the cable keystone angle. The 27-strand cable with a 1 degree keystone angle was chosen for TQ models as a conservative approach.

Heat treatment optimization allowed to find HT cycles that preserved an acceptable I_c, and provided at the same time an I_S larger than magnet operation currents. Short sample limit predictions for the SQ02 model that was tested in the LARP program were obtained using witness samples. These predictions were ~98% accurate with respect to the SQ02 performance.

Based on the results of this work, strand specifications were formulated for next LARP quadrupole models.

REFERENCES

[1] R. Bossert *et al.*, "Development of a 90-mm Nb_3Sn technological quadrupole for LHC upgrade based on SS collar," in *this conf.*, paper WEA07PO08.

[2] S. Caspi *et al.*, "Design and construction of TS01—a 90-mm Nb_3Sn quadrupole model for LHC luminosity upgrade based on a key and bladder structure," in *this conf.*, paper WEA07PO03.

[3] P. Ferracin *et al.*, "Assembly and test of SQ01b, a Nb_3Sn racetrack quadrupole magnet for the LHC accelerator research program," in *this conf.*, paper WEA07PO12.

[4] S. Feher, "Development and Test of Nb_3Sn Cos-theta Magnets Based on RRP and PIT Strands," in *this conf.*, paper TUA2OR4.

[5] D. Dietderich *et al.*, "Correlation between strand stability and magnet performance," *IEEE Trans. Appl. Supercond.*, vol. 15, no. 2, p. 1524, 2005.

[6] A. Ghosh *et al.*, "Dynamic stability threshold in high-performance internal-tin Nb_3Sn superconductors for high field magnets," *Supercond. Sci. Technol.*, vol. 18, pp. L5–L8, 2005.

[7] E. Barzi *et al.*, "Instabilities in transport current measurements of Nb_3Sn strands," *IEEE Trans. Appl. Supercond.*, vol. 15, no. 2, p. 3364, 2005.

[8] ——, "Study of Nb_3Sn cable stability at self-field using a SC transformer," *IEEE Trans. Appl. Supercond.*, vol. 15, no. 2, p. 1537, 2005.

[9] L. T. Summers *et al.*, "A model for the prediction of Nb_3Sn critical current as a function of field, temperature, strain and radiation damage," *IEEE Trans. Magn.*, vol. 27, no. 2, pp. 2041–2044, 1991.

[10] E. Barzi *et al.*, "Study of Nb_3Sn strands for Fermilab's high field dipole models," *IEEE Trans. Appl. Supercond.*, vol. 11, no. 1, p. 3595, 2001.

[11] N. Andreev *et al.*, "Superconducting current transformer for testing Nb_3Sn cable splicing technique," *IEEE Trans. Appl. Supercond.*, vol. 13, no. 2, p. 1274, 2003.

[12] A. Lietzke, "SQ02 Test Report," LBNL Supercon Internal Note, to be published.